

## Austenite Textures in Ni-Ti and Cu-based Shape Memory Alloys

S. Eucken<sup>1</sup>, Institut für Werkstoffe, Ruhr-Universität Bochum, D-4630 Bochum 1 and J. Hirsch<sup>2</sup>, Institut für Allgemeine Metallkunde und Metallphysik, RWTH-Aachen, D-5100 Aachen

### Introduction

The maximum strain which can be obtained in shape memory alloys either for one-way, two-way effects or pseudoelasticity is limited by the crystallography of lattice variant shear of the particular crystallographic system (1-4). This shear may vary between more than 20 degrees for the b.c.c. → f.c.c. or f.c.c. → b.c.c. or f.c.c. → h.c.p. transformations and a few degrees for transformations which imply only slight tetragonal or rhombohedral distortions. Most materials are polycrystals, and this shear occurs inside of grains. The bulk shape change is affected by the orientations of the individual grains and, in addition, by the constraint which each grain experiences by grains in its environment.

Consequently, the maximum transformation shear can only be realized in single crystals with optimal orientation with respect to the external load, which transforms the high temperature phase into a martensitic single crystal. The behaviour of polycrystalline materials will be modified by two parameters: The orientation distribution, i.e. the texture of the polycrystal and the microstructure, predominantly the grain size and shape.

The subject of the present investigation was to find a microstructure which leads to maximum bulk shear in shape memory alloys. For this purpose experiments were conducted to create different textures and grain structures. Two methods are established for the production of semifinished products or parts of shape memory alloys: Conventional casting, plastic deformation and heat treatments or powder metallurgical methods (5,6). They both possess merits and disadvantages. In deformed alloys recrystallization may provide a chance to produce recrystallization textures and defined grain sizes. The powder metallurgical method will predominantly produce a textureless structure and a small grain size which is related to the initial powder size. A third method is the production of bulk material by direct solidification from liquid. For this purpose the meltspinning method was applied. It is known that solidification textures can originate by columnar growth of crystallization fronts (7,8). Textures originated from meltspinning and from conventional processing are analyzed in this paper.

### Materials and Experimental Methods

The chemical composition of the alloys used for this investigation is given in table 1. The conventionally processed Ni-Ti alloy was hot rolled to a thickness of 0.5 mm and recrystallized. Specimen of all of these alloys were induction melted and subsequently meltspun on a copper wheel. The cooling conditions could be modified by choosing different circumferential wheel velocities, ejection pressures and angles between the nozzle and the wheel which, in turn, produce ribbons of variable thickness (5 to 150 μm) and cooling conditions. The microstructure of the ribbons were investigated by light and scanning electron microscopy in order to determine structural homogeneity, grain size and grain shapes.

Subsequently, tensile tests were conducted in the temperature range in which shape memory effects occur in order to determine the extend of the shape changes associated with the

<sup>1</sup> present address: Kantstr. 49, D - 2863 Ritterhude

<sup>2</sup> present address: Fabrication Technology Division, Alcoa Center, Pennsylvania 15069, USA

alloy number	alloy composition	$M_s$ K(°C)	phase at ambient temperature
1	Cu 24.35 wt.% Sn	213 (-60)	austenite
2	Cu 12.8 wt.% Al 3.3 wt.% Ni	353 ( $\approx$ 80)	martensite
3	Ni 50.1 at.% Ti	293 (+20)	austenite

**Table 1:** Composition and phase structure of the alloys

transformation.

The X-ray measurements of textures were carried out on a fully automatic texture goniometer (9) using Cu  $K_\alpha$  radiation.  $\{110\}$  and  $\{200\}$  pole figures were measured from both sides of the ribbons: The bottom surface which was in contact with the cooling wheel and the top surface. Prior to the pole figure measurement the Bragg angles  $\theta_i$  were determined indivi-



**Fig. 1:** Scanning electron microscopy of specially prepared (11) ribbons cross sections: a) equiaxed grain structure, occurs at slower cooling rates, b) columnar grain structure, occurs at high cooling rates

dually for each material by a  $\theta/2$  scan. Only the reflection mode was applied with a maximum tilting angle  $\alpha = 85^\circ$ . The corrections for background intensity and defocussing effects were taken from off-Bragg angle measurements (separately measured for each sample) and from the evaluation of the  $\alpha$  dependent intensities of a reference sample (with random texture).

### Experimental Results

Scanning electron microscopy of for this purpose mercury embrittled fracture surfaces showed that principally two different types of homogeneous microstructure were obtained in the hot rolled and meltspun alloys equiaxed and columnar grains (Fig. 1).

All alloys are obtained as homogeneous ordered b.c.c. phases, the structure of which has been described in earlier papers (10).

The textures of the Cu-based alloys investigated in high temperature ordered bcc austenite phase are shown in Figs. 2 and 3 in form of a)  $\{110\}$  and b)  $\{200\}$  pole figures, each measured from the upper side (top side: t) and lower side (bottom side: b, i.e. the one which was in contact with the copper wheel), respectively.

Fig. 2 shows the polefigures typical for the columnar microstructures of alloy 1. For this ribbon (Figs. 2a-d) a rather distinct texture is found with the character of a fibre texture, especially pronounced for the upper side ("t", Fig. 2a) where an intensity maximum of 2.6 times random occurs in the  $\{100\}$  and 5.8 times random in the  $\{200\}$  (Fig. 2c) pole figure. The high intensity of the latter is due to the fact that the fibre axis is a  $\langle 200 \rangle$  axis, tilted  $\sim 12^\circ$  from the sheet plane normal (centre of the pole figure) towards the negative reference direction RD, which indicates the rotation direction of the copper wheel. The texture of the lower side "b" (Fig. 2b and d) is similar to "t", but also shows characteristic differ-

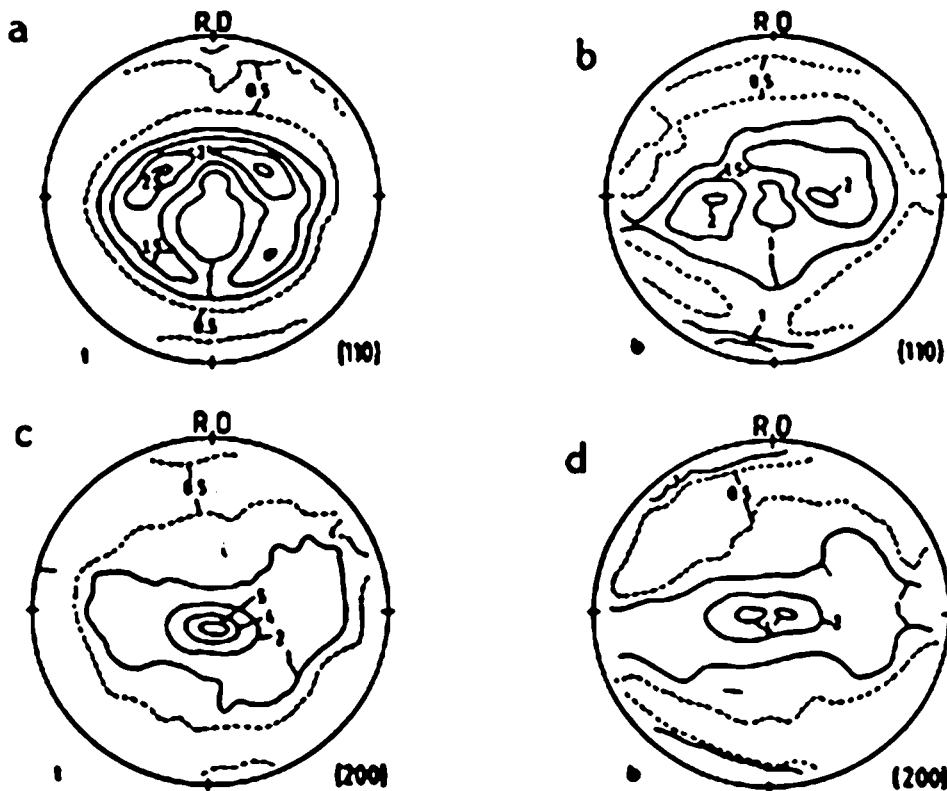


**Fig. 2:** Polefigures of an alloy 1 ribbon with columnar grain structure: a)  $\{110\}$  pole figure of top surface, b)  $\{110\}$  of bottom (contact) surface, c)  $\{200\}$  of top surface, d)  $\{200\}$  of bottom surface

ences. It is less pronounced (2.1 and 4.9 times random) and it appears to be more symmetric than 1-t showing no shift of the {200} fibre axis towards RD. (Both textures show a certain scattering along the equator line, to the left and to the right, i.e. by rotation around RD.) This, however, should not be overestimated since it was rather difficult to adjust the small ribbon in an exact horizontal position to the measured surface, which might cause such an effect.

The textures of alloy 1 ribbon with an equiaxed grain structure (Fig. 3a-d) are much weaker with maximum intensities of 1.6 times random in both {110} pole figures and 2.2 or 2.8 in the {200} pole figure. Thus here the textures appear to be closer to random and no distinct fibre axis occurs in the {200} pole figure.

Typical results of tensile tests are shown in Fig. 4: In Cu-based alloys the textured material deforms to a much higher degree as compared to the equiaxed random structure. In addition the stress to induce the transformation strain is higher for the random orientation.

The  $\langle 110 \rangle$  fibre texture of the hot rolled and recrystallized Ni-Ti alloy is a typical recrystallization texture for bcc alloys (Fig. 5). Meltspinning of NiTi requires involved efforts (described in (12)) because of the high reactivity of the molten alloy. The columnar microstructure can be obtained over a wide range of meltspinning conditions as well and a strong  $\langle 100 \rangle$  fibre texture was usually found in the  $\beta$  phase (Fig. 6). Only at one time a double fibre texture  $\langle 100 \rangle$  and  $\langle 110 \rangle$  was yet observed (Fig. 7).

Shape memory effects of more than 9 % and fracture strains of 18 % were observed in hot rolled and recrystallized NiTi. In the  $\langle 100 \rangle$  fibre textured ribbons the shape memory strain was up to 5 % and the fracture strain 7.5 % (12).

## Discussion

In the meltspun alloys an understanding of the two types of microstructure can be based on different types of nucleation of crystals. The columnar grains nucleate at the interface between liquid and the wheel and grow through to the upper surface. The sharpening of the texture can be explained by growth selectivity of the [100] orientation (13). The deviation of the fibre axis at the upper surface can be understood by the fact that the wheel is moving while the crystal is growing. Equiaxed grains should originate most likely by individual probably heterogeneous nucleation of grains in the interior of the melt.

The effect of texture on the bulk transformation induced strain in Cu-based alloys is shown in figure 4. The columnar grain structure grows about perpendicular to the length of the ribbon which is exposed to a tensile stress. In loading direction [100] and [110] orientations are dominating because of the texture. It is well known that martensitic shear occurs in a (110) [110] shear system. Cube texture or to a somewhat lesser degree cube fibre texture provides the optimum orientation for maximum shear stress in this particular shear system. In addition, the columnar structure creates favourable conditions for minimum constraint of the interfaces. Therefore values for the bulk shape change can be obtained which approach the theoretical value for  $\beta$ -Cu base alloys (14) which would be obtainable only by single crystals of optimum orientation. On the other hand, the equiaxed microstructure on average crystallizes with a less favourable orientation. A smaller shear stress is acting in the direction of the shear transformation tensor. A high constraint exists, as given by the fact that most of the grains are surrounded by other grains which impede their individual shape change.

The role of texture in shape memory alloys has been analyzed in (15): The initial orientation distribution can be favourable or random with respect to phase transformation. There are 12

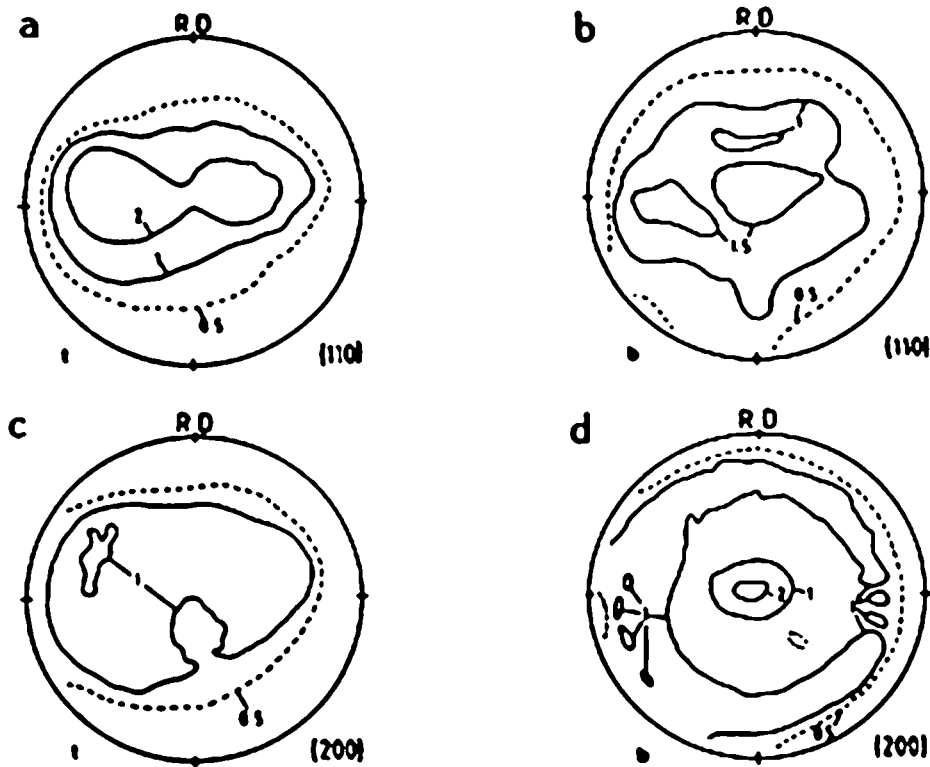


**Fig. 3:** Polefigures of an alloy 1 ribbon with equiaxed grain structure, a)  $\{110\}$ , top surface, b)  $\{110\}$ , bottom surface, c)  $\{200\}$ , top surface, d)  $\{200\}$ , bottom surface

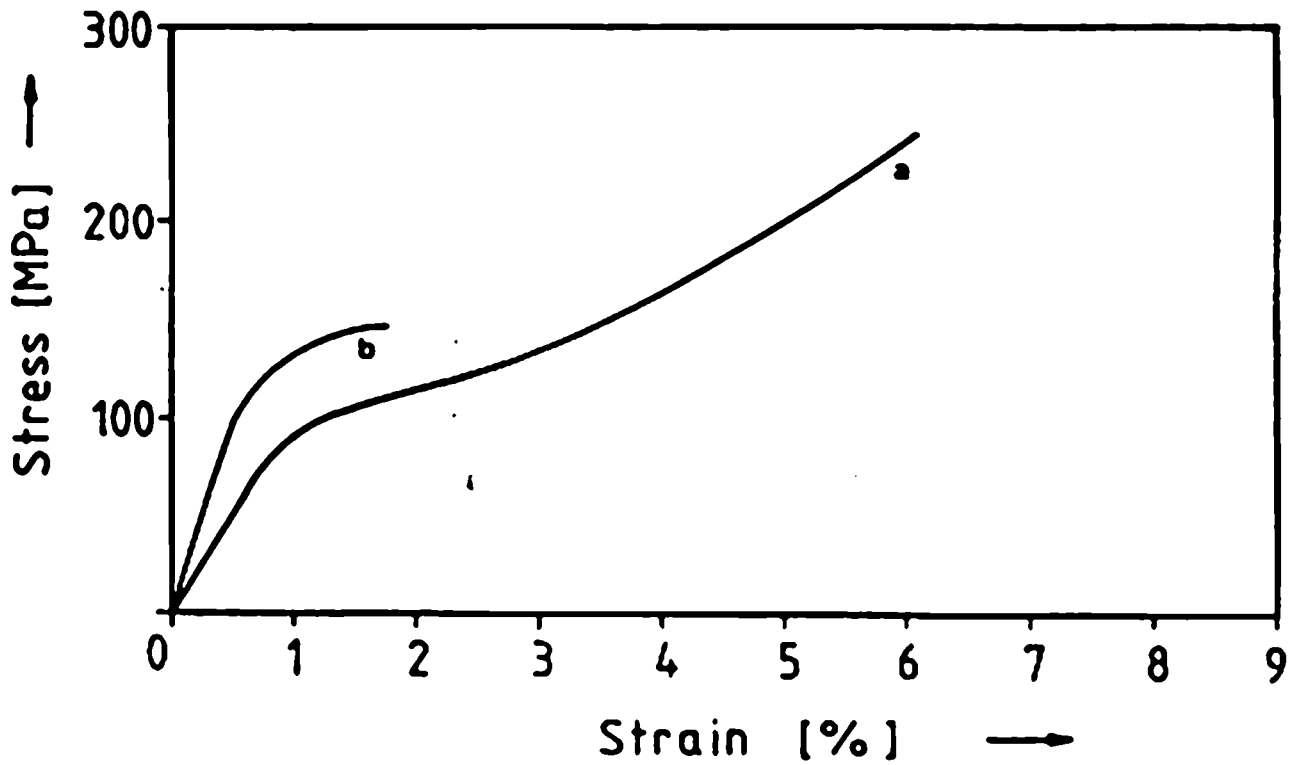


**Fig. 4:** Tensile testing of Cu-Al-Ni ribbon with columnar (a) and equiaxed (b) grain structure

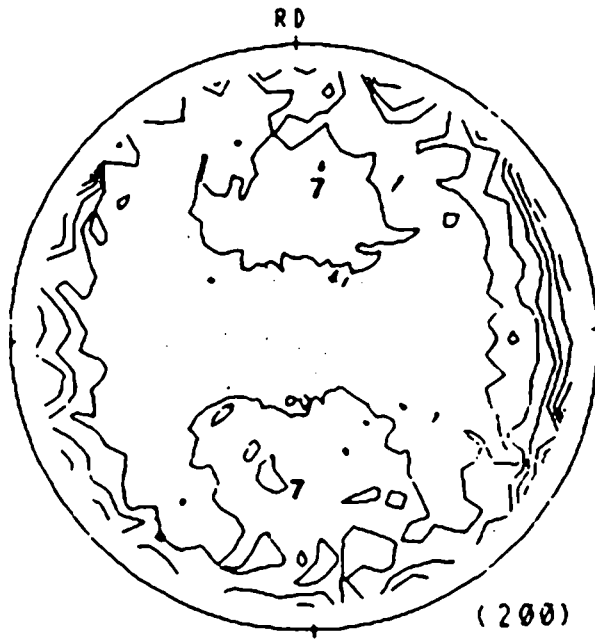


**Fig. 5:** Recrystallization texture of hot rolled NiTi

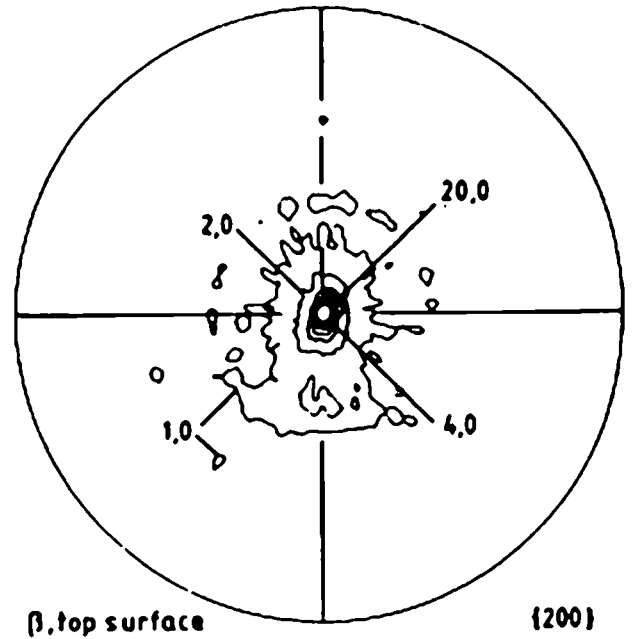


**Fig. 6:**  $\langle 100 \rangle$  fibre texture in a meltspun NiTi ribbon

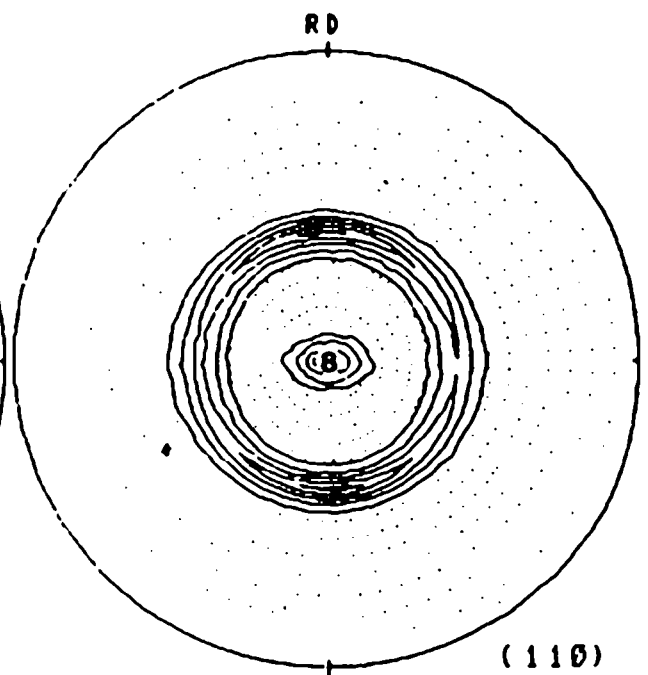
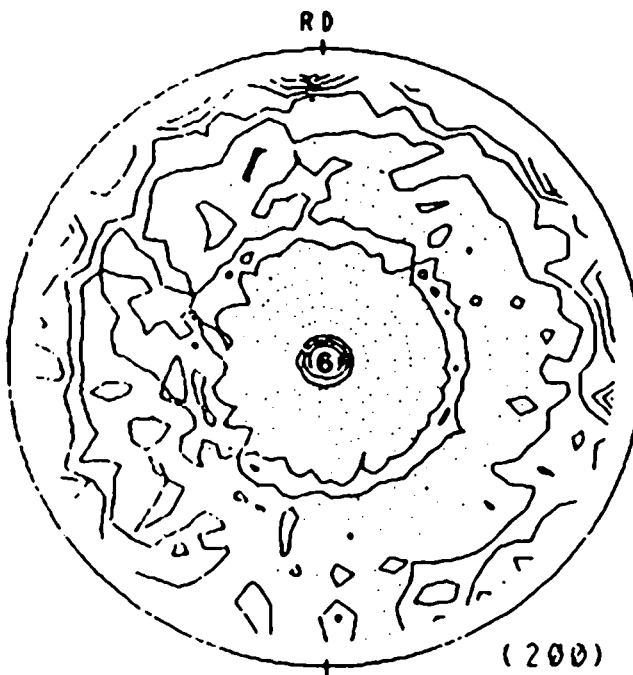


**Fig. 7:**  $\langle 100 \rangle$  Exceptional double fibre texture  $\langle 110 \rangle$  and  $\langle 110 \rangle$  in an NiTi ribbon produced by meltspinning

equivalent  $\{110\} \langle 1\bar{1}0 \rangle$  shear systems for the transformation into martensite. Consequently a further randomization will occur in either the original random or the textured material if the transformation takes place without external shear stress.

If the transformation occurs under stress final saturation conditions will be defined by the fact that only the one, the most favourable, shear system will be left to transform the material. In this case the material containing favourable texture will be transforming into a pronounced new texture which can be directly derived from the crystallography of lattice variant shear. Each grain of the originally random material will also transform into martensite of unique orientation, which however will inherit the scatter of the original  $\beta$  grains. As a consequence in average these grains will also contribute less shape change by shear in direction of the external tensile load. The texture obtained by columnar growth has proved to be an orientation favourable to stress affected phase transformation. There is a possibility that less favourable orientations exist. In such a case the shape change could be less even than that which is obtained by the textureless random material.

In NiTi the dependency of strain from crystal orientation is completely different (16): The largest shape memory strains are observed between  $[111]$  and  $[110]$  orientations in single crystals with more than 10.5 % while  $[100]$  is the most unfavourable orientation with 3 % strain only. The recrystallization texture offers favourable orientations in tensile axis while the mixture of  $[100]$  and  $[110]$  orientation in tensile axis of the meltspun Ni-Ti ribbons could not show much more than 5 % shape memory strain. The  $\langle 100 \rangle \langle 110 \rangle$  double fibre texture may be a first step to more favourable textures in meltspun NiTi. Perhaps rolling and recrystallization of the ribbons could optimize the shape memory behaviour. Nevertheless, it was shown that the reversibility of shape memory strain can even be better in textured ribbons prepared by meltspinning (12) compared to conventionally produced NiTi.

Our work has shown that the actual bulk deformation of shape memory alloys  $\epsilon \approx 2\gamma$  can be affected by three factors:

1. the texture of the  $\beta$  phase
2. the grain size of the material and
3. (as it is well known) the amount of external stress.

The optimum shape memory shear is represented by coarse grain material with optimum texture. It has to be exposed to the critical stress which provides the shear stress sufficient to complete selectivity of the shear systems.

### Acknowledgement

The support of the German Science Foundation (DFG project Ho 325/21) is gratefully acknowledged.

### References

- (1) C. M. Wayman, Introduction to the Crystallography of Martensite Transformations, Macmillian Company, New York (1964).
- (2) K. Otsuka and K. Shimizu, International Metals Reviews (1986) 93.
- (3) E. Hornbogen and G. Wassermann, Z. Metallkde 47 (1956) 427.
- (4) G. Wassermann, Arch. Eisenhüttenwes. 10 (1936/37) 321.
- (5) R. Elst, J. van Humbeck, M. Meeus and L. Delaey, Z. Metallkde 77 (1986) 421.
- (6) T. W. Duerig, J. Albrecht and G. H. Gessinger, J. of Metals (1982) 14.
- (7) W. M. Stoobs and J. V. Wood, Acta Met. 27 (1979) 575.
- (8) S. Eucken, Schmelzspinnen von Legierungen mit Formgedächtnis, VDI-Fortschrittberichte, Reihe 5, Nr. 119, VDI-Verlag, Düsseldorf (1987).

- (9) J. Hirsch, G. Burmeister, L. Hoenen and K. Lücke, in: *Experimental Techniques of Texture Analysis* (ed. by H. J. Bunge), DGM-Verlag, Oberursel (1986) p. 63.
- (10) S. Eucken and E. Hornbogen, in: *Rapidly Quenched Metals* (ed. by S. Steeb and H. Warlimont), Elsevier Science Publisher B.V., Amsterdam (1985) p. 1429.
- (11) C. Caesar and U. Köster, in: *Rapid Solidification of Crystalline Alloys* (ed. by J. V. Wood), The Institute of Metals, London (1988) in print.
- (12) S. Eucken, G. Otto, P. Donner und S. Justi, *Proceedings 6th World Conference on Titanium, Cannes, Les Editions de Physique, Les Ulis (Cedex France) (1988) in print.*
- (13) G. Wassermann and J. Greven, *Texturen metallischer Werkstoffe*, Springer Verlag, Berlin (1962).
- (14) J. de Vos, L. Delaey, E. Aernoudt and P. van Houtte, in: *Proc. 3rd Int. Conference Martensitic Transformation* (ed. by W. S. Owen), Cambridge, Massachusetts (1979) p. 148.
- (15) S. Eucken, J. Hirsch and E. Hornbogen, *Textures and Microstructures* 8 & 9 (1988). 415.
- (16) S. Miyazaki, S. Kimura, K. Otsuka and Y. Suzuki, *Scripta Met.* 18 (1984) 883.